

## TOWARDS DATA-DRIVEN MODELING OF PATHOLOGICAL TREMORS

**Jiamin Wang, Sunit K. Gupta , Oumar Barry\***  
 Department of Mechanical Engineering  
 Virginia Polytechnic Institute and State University  
 Blacksburg, Virginia 24061

### ABSTRACT

*Understanding the dynamics of pathological tremors (e.g., Parkinson's Disease, Essential Tremor) is crucial to developing effective treatments for these neurological disorders. This paper studies the data-driven modeling of periodic and quasiperiodic tremors. A general neuromusculoskeletal model is proposed to serve as the theoretical basis of this study. The Parkinsonian tremor data is first observed in terms of periodicity, frequency composition, and chaotic characteristics, which confirm tremor is a nonlinear dynamics problem. Two data-driven models are then proposed to predict the nonlinear dynamics of tremor: (1) a model-free approach via long short-term memory recurrent neural network, and (2) a model-based approach via extended dynamical mode decomposition. These models are compared to existing models and the results show that the proposed models outperform existing models for long term prediction of tremor.*

### NOMENCLATURE

The mathematical notations used are listed as following:

- $\|Z\|_n$  The induced  $n$ -norm of a matrix  $Z$  ( $n = 2$  if not specified)
- $z_1 \times z_2$  Multiplications of quaternions  $z_1$  ( $4 \times 1$ ) and  $z_2$  ( $4 \times 1$ )
- $\bar{z}$  Conjugation of quaternion  $z$  ( $4 \times 1$ )
- $z_{m \times n}$  A  $m \times n$  matrix with all elements as  $z \in \mathbb{R}$  (fits along with its neighboring blocks if no dimension specified)
- $I_n$  Identity matrix of a specific dimension  $n$  (fits along with its neighboring blocks if no dimension specified)
- $Z^{-T}$  The transposed inverse of  $Z$  (since  $(Z^{-1})^T = (Z^T)^{-1}$ )
- $Z^+$  The Moore-Penrose pseudo inverse of  $Z$

### INTRODUCTION

Activities of daily life such as writing, eating, and object manipulation are extremely difficult for patients suffering from pathological tremors. Parkinson's Disease (PT) [1] and Essential Tremor (ET) [2] are the two most common disorders marked by tremors and affect millions of people around the world. Tremors are generally summarized as involuntary, rhythmic, and oscillatory movements [3]. The common frequency of PT and ET are 3~6 Hz [1] and 4~12 Hz [2], respectively. Research has indicated that the observed tremorous movements may contain components from the central neural oscillator, the peripheral neural feedback/reflex resonance, and the mechanical resonance [3, 4].

A thorough understanding of the dynamics of pathological tremors will facilitate the classification and diagnosis between different tremors [5], as well as improve the design of prediction algorithms adopted in electrical stimulation [6, 7] and rehabilitation orthoses [8–10] for tremor suppression. Existing real-time tremor prediction algorithms are developed based on harmonic/frequency and time delay models such as Weighted-Frequency Fourier Linear Combiner (WFLC) [11], Band-limited Multi-frequency Fourier Linear Combiner (BMFLC) [12], and Autoregressive model (AR) [13]. However, the structures of these models are too general and simple to accurately predict tremors in the long term. On the other hand, many studies conducted the modeling the musculoskeletal systems [14, 15], neuromuscular systems [16, 17], and the combination of both [18, 19]. However, particularly in tremor studies [19, 20], either some of the adopted models are simplified, or the approaches are limited to linear models and analyses. These unsolved problems have motivated us to explore a better model for accurate long term

---

\*Corresponding Author (Email: obarry@vt.edu)

tremor prediction and nonlinear analysis.

In this paper, we studied the data-driven modeling of periodic and quasiperiodic tremor signals. A general neuromusculoskeletal model has been proposed as the fundamental setup for the analysis. Acquired from a PT database [21], the tremor data measured in movements has been examined numerically in periodicity/chaoticity and frequency composition. The observations confirmed that tremor is a nonlinear problem. The limitations of the existing tremor prediction algorithms led to our exploration of data-driven modeling of the PT tremor. Under certain model assumptions, the regression and prediction of periodic and quasiperiodic tremors are carried out with model-free and model-based methods. The modeling results based on different methods are compared and discussed. Finally, the conclusion section summarizes the findings and discusses future research directions.

## A GENERAL NEUROMUSCULOSKELETAL MODEL

Neuroscience studies have shown that the motor cortex signal can be decoded to predict hand movement [22]. Therefore, if tremor signal originates anew in the cortical neural system, the resulting tremorous movement can be considered as a system response from an excitation source. Previous works also indicate the involvement of feedback/reflex loop (e.g., Golgi Tendon Organs, Renshaw Cells, Spindle Organs) in pathological tremor [19]. These subsystems in the nervous system are highly coupled. The dynamics of tremor may be related to the time delay of signals in the system as well [23]. It is noticed that the PT tremor may involve limit cycle behaviors resembling the effects of time delay [24,25]. To thoroughly investigate the role of these factors in pathological tremor dynamics that involve excitation, feedback loop, and delay, a general nonlinear dynamical model of the human forearm can be established as

$$x = \begin{bmatrix} q \\ \dot{q} \\ \tau \\ \eta \\ \xi \end{bmatrix}; \quad \dot{x} = f(x_{t,i}, \gamma, w) = \begin{bmatrix} \dot{q} \\ f_a(q, \dot{q}, \tau, u, \xi, w_a, \theta_a) \\ f_\tau(q, \dot{q}, \tau, \eta, w_\tau, \theta_\tau) \\ f_\eta(q, \dot{q}, \tau, \eta, \gamma, w_\eta, \theta_\eta) \\ f_\xi(q, \dot{q}, \tau, \xi, \theta_a) \end{bmatrix} \quad (1)$$

with

$$f_\tau = f_{\tau,0}(q, \dot{q}, \tau, \eta, w_\tau, \theta_\tau) + \sum_{i=1}^m f_{\tau,i}(q_{t,i}, \dot{q}_{t,i}, \tau_{t,i}, \theta_\tau)$$

$$f_\eta = f_{\eta,0}(q, \dot{q}, \tau, \eta, \gamma, w_\eta, \theta_\eta) + \sum_{i=1}^n f_{\eta,i}(q_{t,i}, \dot{q}_{t,i}, \tau_{t,i}, \eta_{t,i}, \theta_\eta)$$

where  $f_a$ ,  $f_\tau$ , and  $f_\eta$  are respectively defined as the multibody system (MBS) that contains the forearm skeletal system and exoskeleton system, the neuromuscular system (NMS), and the peripheral nervous system (PNS) [19];  $q$  is the generalized coordinates in MBS;  $\tau$  is the torque that also reflects the musculotendon dynamics;  $\eta$  is the neuromuscular signal;  $\gamma$  is the cortical neural signal;  $\xi$  is the internal state from human tissue and soft material;  $u$  is the exoskeleton actuation input;  $w$  is the perturbation and disturbance vector; and various  $\theta$  are the model parameters. Note that the states with the subscript are defined as  $x_{t,i} = x(t - t_i)$ ,

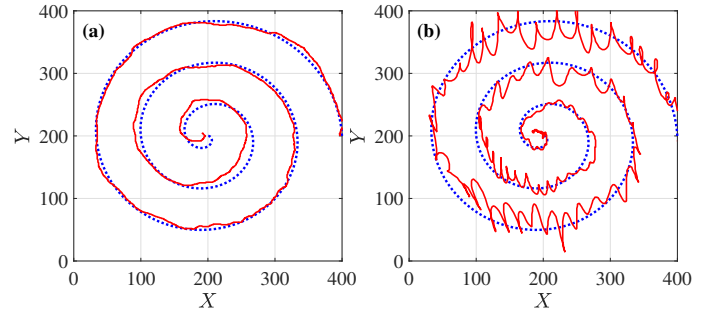


**FIGURE 1:** Archimedean spiral drawing from (a): a health subject, and (b): a PT patient subject. The blue dot lines are the reference, and the red solid lines are the trajectories.

where  $t_i$  is the time delay that occurs in the neural signals.

A detailed study of this general model will provide a better understanding of the mechanism of tremor. Identifying such a system requires observation and data collection of the states over a period of time. As some of the studies have pointed out that the behaviors of tremor signals are affected by the posture and movement [20], an exclusive dynamical model regression can be very challenging. However, in cases such as voluntary motion is static or slowly periodic, model assumptions can be made to simplify the scope of the problem. Further explanation of the assumptions will be provided in later sections.

## TREMOR DATA AND OBSERVATIONS

In this study, we evaluated the data from the tremor database in [21]. The tremorous motion data sets were recorded from PT patients with a pair of tablet and stylus. The data was collected when the patients were performing Archimedean spiral drawing (shown in Fig.1) and point tracking (holding the stylus above a static point without touching the tablet). When the stylus is touching the tablet, the natural human movements will be constrained. The resolution of the translational position measurement is also lower than that of the stylus attitude - the angle between the stylus and normal vector of the tablet screen. Therefore, we mainly focused on the stylus attitude data from point tracking tests. Note that by giving the orientations of the pen and the tablet respectively as quaternion vectors  $\xi_1 \in \mathbb{R}^4$  and  $\xi_2 \in \mathbb{R}^4$  in the global frame, the attitude measurement can be expressed as

$$y = 2 \arccos \left( [1 \ 0_{1 \times 3}] (\xi_1 \times \bar{\xi}_2) \right) \quad (3)$$

which contains the coupled information of the 3D rotations.

Even when the measurements do not provide the full information of 3D rotation, they still demonstrate the signature features of PT tremor. Figure 2 demonstrates the tremorous motion in the attitude from four of the point tracking tests. The sampling rates of these measurements are approximately 140 Hz. The data has also been low-pass filtered by a zero-phase 5th order infinite impulse response (IIR) filter at 20 Hz. The oscillations demonstrate some repetitive patterns and resembling features. We also

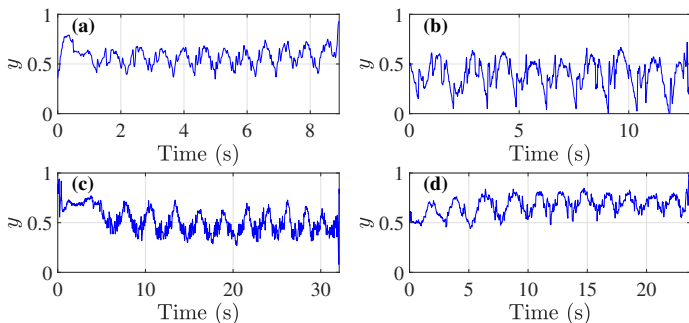


**FIGURE 2:** Demonstration of tremors in  $y_1$  collected from point tracking tests involving PT patients. Time series in (a), (b), (c), and (d) are collected from different experimental trails.

notice that there is distortion in amplitude, period, and frequency composition between each similar segment. For instance, we specifically examined the trajectory in Fig.2(b). The signal here is further high-pass filtered at 3 Hz. The results are shown in Fig.3. It can be clearly noticed that the green ( $t \in [4.8, 6.2]$  seconds) and cyan ( $t \in [6.2, 7.5]$  seconds) parts of the tremor signal in Fig.3(a) share a periodic-like pattern. The autocorrelation in Fig.3(b) indicates such pattern appears approximately every 1.33 seconds. Finally, in Fig.3(c), the spectrogram of the signal reveals that tremor consists of multiple harmonic components that shift in frequency and magnitudes. The dominant frequency is around  $4 \sim 5$  Hz.

As preparation for tremor modeling and analysis, we have also produced periodic and quasiperiodic tremor signals. By replicating the green signal segment ( $t \in [4.8, 6.2]$  seconds in Fig.3(a)) in the time domain, two tremor signals  $y_1$  and  $y_2$  are

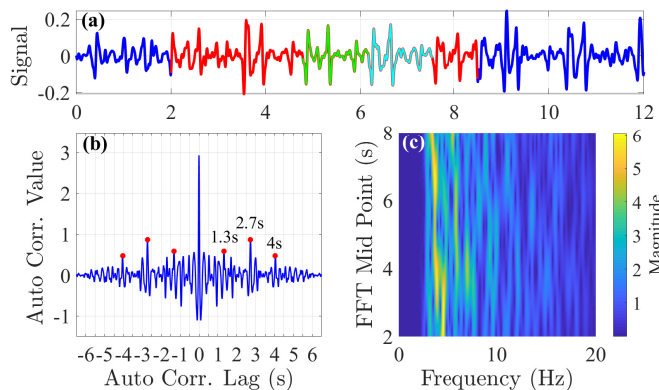


**FIGURE 3:** Analysis of the tremor trajectory in Fig.2(b), where (a) demonstrates the periodic-like pattern in the red part of the signal in the range of  $t \in [2, 8.5]$  seconds, which is especially noticeable between the green ( $t \in [4.8, 6.2]$  seconds) and cyan ( $t \in [6.2, 7.5]$  seconds) part; (b) shows the autocorrelation plot of the red part; and (c) shows the spectrogram of the red part. The horizontal axis in (a) is time in seconds.

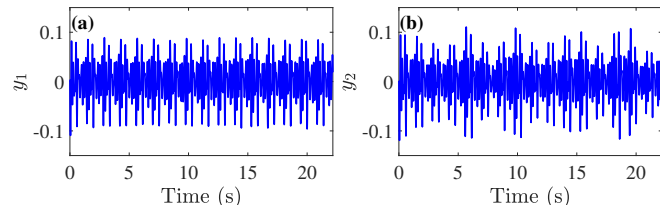


**FIGURE 4:** The time trajectories of the stochastic periodic signal  $y_1$  in (a), and the stochastic quasi-periodic signal  $y_2$  in (b).

generated based on the equation

$$y_i(t) = g_a(t)y_0(t) + w_y(t); \quad (4)$$

where  $i$  is the labeling number;  $y_0$  is the extended green signal, which is periodic;  $g_a$  is the amplitude shift function that scales the tremor signal; and  $w_y$  is normally distributed random noise. The trajectories of the signals are shown in Fig.4. Note that  $y_1$  is set to be stochastic periodic by having  $g_a(t) = 1$ , and  $y_2$  is set to be stochastic quasiperiodic by having  $g_a(t) = \sin(\sqrt{2}t) + \cos(2t)$ . This is to ensure that  $y_1$  and  $y_2$  preserve their dynamical features shown in the original signal. The scope of the current study is limited to periodic and quasiperiodic responses, since true chaotic behaviors are sensitive to initial conditions, and cannot be generated by transforming  $y_0$  from Eq.(4) into a time-dependent periodic signal.

It cannot be confirmed from the current numerical data whether tremor is also chaotic. We attempt to numerically examine the Lyapunov exponent of both the original tremor signal and the stochastic periodic signal  $y_1$ , based on the algorithm by Rosenstein [26]. In brief, the algorithm estimates the maximal Lyapunov exponent (MLE) from the infinitesimally close trajectories of a discrete-time signal in its time-delayed phase space. The average logarithmic divergence of the original signal and  $y_1$  is shown in Fig.5. MLE can be estimated as the slope from the linear regression of a single plot, where a positive MLE indicates chaos. However, the algorithm appears to be sensitive to noise, and incapable of distinguishing chaoticity from stochastic periodicity. This is indicated in Fig.5(b), demonstrating that  $y_1$  is chaotic. Also, in both subfigures, none of the plots calculated

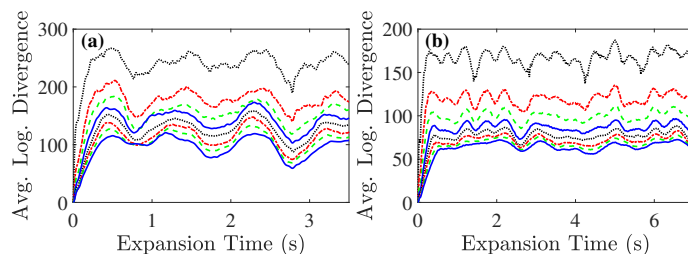


**FIGURE 5:** The plots of average logarithmic divergence calculated from the algorithm by Rosenstein [26], where (a) shows the plots for the original tremor signal, and (b) shows the plots for the stochastic periodic signal  $y_1$ . In each of the subfigures, the eight plots ranked from high to low in divergence have embedding dimension ranging from 3 to 10, respectively.

at different embedding dimensions demonstrate a steady divergence or convergence over time.

The above observations confirm that tremor is a complicated nonlinear dynamics problem. The later section will discuss the data-driven modeling of tremor based on the signals in Fig.4.

## DATA-DRIVEN MODELING OF TREMOR

As mentioned in the Introduction section, a variety of algorithms has been developed for tremor prediction. The algorithms constructed on general harmonic or time delayed models are mainly designed for real-time prediction. The discrete-time formulation can be expressed as

$$\begin{aligned}\theta_k &= \theta_{k-1} + w_{\theta,k}; \\ y_k &= h_z(t, \theta_k, y_{k-i}) + w_{z,k}, \quad (i = 1, 2, \dots, n)\end{aligned}\quad (5)$$

where  $k$  is the discrete time,  $\theta$  is the model parameter that is incorporated as the states, which are assumed to be constant; and  $w$  are disturbance/noise in the state and measurement. The extended Kalman filter (EKF) [27] for parameter update can then be written as

$$\varepsilon_{y,k} = y_k - h_z(t, \theta_k, y_{k-i}) \quad (6)$$

$$G_k = P_{k-1} H_k^T (H_k P_{k-1} H_k^T + R) \quad (7)$$

$$\theta_k = \theta_{k-1} + G_k \varepsilon_{y,k} \quad (8)$$

$$P_k = (I - G_k H_k) P_{k-1} + Q \quad (9)$$

where  $\varepsilon_y$  is the estimation error;  $Q$  and  $R$  are the process and measurement noise covariance;  $P$  is the predicted covariance estimate; and  $H_k = \partial h_z / \partial \theta_{k-1}$  is the Jacobian of the nonlinear observation with respect to the parameters.

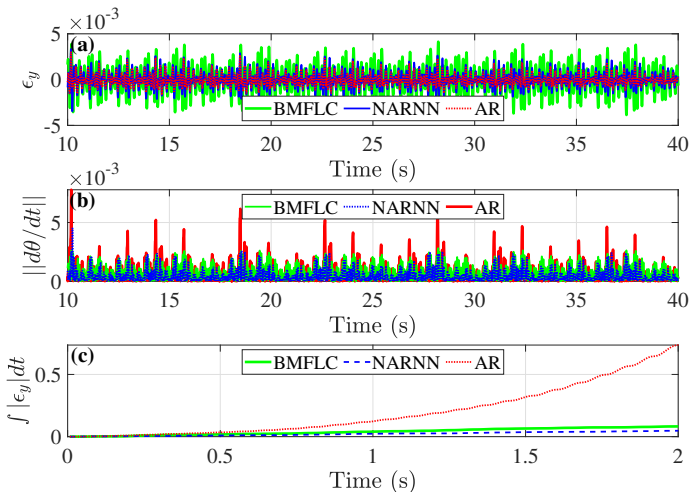


**FIGURE 6:** Online tremor regression and prediction with BMFLC, NARNN, and AR models implemented with EKF, where (a) shows the one-step prediction error of quasiperiodic signal  $y_2$ ; (b) demonstrates the norm of parameter updates along time; and (c) presents the integral of long term prediction error norm in 2 seconds.

Simulations are carried out to demonstrate the performance of one-step predictions from existing models (AR [13] and BMFLC [12]), and a nonlinear autoregressive neural network (NARNN) designed by the authors. The BMFLC covers a band between 1 ~ 15 Hz with a resolution of 0.1 Hz; the AR and NARNN use time-delayed measurements  $y_{k-i}$  with  $i$  up to 5; and the NARNN has one feedforward hidden layer with 3 neurons. The result in Fig.6(a) shows that all three models are effective in the one-step prediction. It should also be noted that BMFLC has two advantages - it does not require filtering the signal, and it can be directly included in an adaptive controller [10]. However, BMFLC only works well when its bandwidth precisely covers the frequency components of a periodic/quasiperiodic signal.

For real-time prediction, it is preferable that the dynamics of the signal is precisely described by a simple model. However, from Fig.6(b), it is clearly shown that none of the models can accurately regress the tremor signal in the long run since their model parameters are constantly changing due to underfitting. Figure 6(c) shows that an unstable prediction model may even lead to unbounded prediction error if its parameters are not adaptive. Long term prediction, however, can significantly improve tremor suppression performance in applications, since they can compensate the time lag during signal communication and calculation process. The limitation of existing models also prevents them from being used for nonlinear analysis.

Hence, there exists a need for developing better dynamical models for pathological tremors. Recall that Eq.(1) presents a multi-dimensional system that involves external input and time-delay. While the existing measurement only reveals very limited information, the following assumptions are made for modeling:

- (A1) During the point tracking motion, human intention is considered fixed. In this case,  $\gamma$  is approximated as  $\gamma \approx \gamma^*(x, w)$ , which is a feedback term of  $x$  and  $w$ . This leads to a time-delayed self-excited system  $\dot{x} \approx f(x, \gamma^*(x, w), w) = f^*(x, w)$ , which is stochastically automatic.
- (A2) The signal  $y_1$  and  $y_2$  are respectively the periodic and quasiperiodic solutions of  $\dot{x} = f^*(x, w)$  under certain state and parameter conditions.

Particularly, assumption (A1) is considered for the cases of resting and postural tremors [1, 2], where it is presumed that the cortical signals  $\gamma$  are affected by the neuromusculoskeletal states  $x$  and disturbance  $w$  [28]. These assumptions allow us to study the modeling of tremor in a limited scope based on  $y_1$  and  $y_2$ . The model-free and model-based regression of tremor dynamics are then carried out, which are discussed in the upcoming subsections.

Model-free regression of tremor dynamics is useful for prediction. These models are hard to analyze since it is hard to interpret the physical meaning of the dynamic terms. The benefit of the model-free approach is that it does not require the knowledge of any specific structure. If a time series is successfully

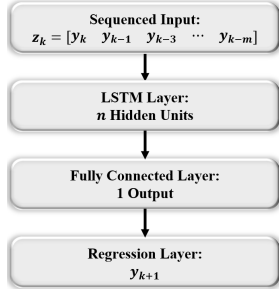


**FIGURE 7:** The structure of LSTM-RNN.

regressed, the scale of the model can also serve as an indication of the complexity and dimensionality of the system.

Long short-term memory recurrent neural network (LSTM-RNN) is suitable for time series regression since they are good at processing data sequences [29]. The structure of the neural network model implemented in this study is shown in Fig.7. The structure contains an LSTM layer with  $n$  hidden units and a fully connected layer. The sequential input  $x_{NN}$  of the model is a  $m+1$  dimensional time-delayed vector

$$z_{NN} = [y_k \ y_{k-1} \ y_{k-2} \ \cdots \ y_{k-m}]^T \quad (10)$$

and the output is  $y_{NN} = y_{k+1}$ .

The performance of LSTM-RNN is shown in Fig.8. Different hidden unit and input dimensions are used for periodic and quasiperiodic signals - for  $y_1$ ,  $m = 30$  and  $n = 100$ ; and for  $y_2$ ,  $m = 300$  and  $n = 700$ . For both trajectories, the networks can capture the dominant features and perform long term predictions. The maximum errors of the predictions are all below  $1.35 \times 10^{-2}$ . An important observation is that for quasiperiodic signals, the complexity of the model is significantly higher since the signal has more features. In this case, if the input sequence is not long enough, the network will end up producing a periodic signal.

The two regression models also indicate that if the signal  $y_1$  or  $y_2$  is the self-excited solutions of a system, the systems will likely have dozens of dimensions that include the neuromusculoskeletal states and their delays. However, since the features learned by LSTM-RNN is likely latent, the network cannot eas-

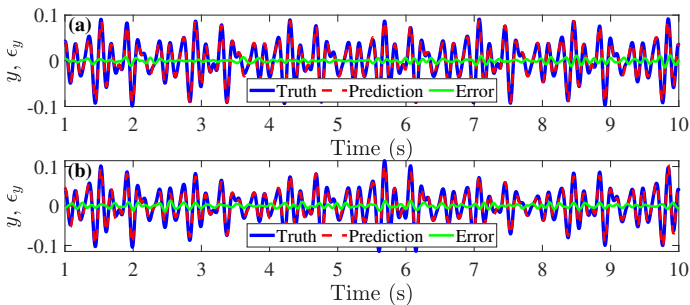


**FIGURE 8:** Prediction of tremor trajectory with LSTM-RNN in a 10-second window, where (a) and (b) shows the prediction and error of  $y_1$  and  $y_2$ , respectively.

**TABLE 1:** EDMD modeling setups, where Dim. is the total state dimension, and Rd. Order is the state order after model reduction.

Label	Signal	$m$	Dim.	Rd. Order	Energy
EDMD	$y_1$	750	3750	50	91.1%
DMD	$y_2$	3750	3750	100	99.9%
EDMD-1	$y_2$	750	3750	100	96.1%
EDMD-2	$y_2$	900	4500	100	91.5%

ily imply physically meaningful information.

To explore the dynamical model of tremor analytically, we employed extended dynamic mode decomposition (EDMD) [30]. EDMD is the nonlinear version of dynamic mode decomposition (DMD) developed based on Koopman analysis, which is applicable to the reduced order modeling of periodic and quasiperiodic systems, in particular, nonlinear partial differential equations (PDE) systems [30]. EDMD adopts a rich set of state observation at time  $t$  that can be written as

$$z_k = [y_k \ y_{k-1} \ y_{k-2} \ \cdots \ y_{k-m} \ \dot{y}_k \ \dot{y}_{k-1} \ \dot{y}_{k-2} \ \cdots \ \dot{y}_{k-m}]^T$$

$$Z_k = \begin{bmatrix} z_k & z_{k-1} & z_{k-2} & \cdots & z_{k-n} \\ h(z_k) & h(z_{k-1}) & h(z_{k-2}) & \cdots & h(z_{k-n}) \end{bmatrix} \quad (11)$$

where  $h(z_k)$  is the nonlinear observer function of  $z_k$  (which is omitted in DMD). Note that since we have little knowledge of the time-delayed properties,  $Z$  is constructed by treating  $f^*$  as a delay differential equation, which is also a class of PDE with a discrete time delay dimension of  $m$ . In the current study,  $h(z_k)$  is selected as the square and cube terms of  $z_k$ , so that the model coefficients corresponding to  $h(z_k)$  can be interpreted as nonlinear stiffness and damping.

When  $m$  is large,  $Z$  will become an extremely large matrix with over thousands of columns. However, the energy in the majority of the states may not be dominant. Proper orthogonal decomposition (POD) based on singular value decomposition (SVD) is then carried out to reduce the order of the model while keeping most of the energy:

$$Z = V\Sigma W^T \approx \check{V}\check{\Sigma}\check{W}^T \quad (12)$$

where  $\check{V}$ ,  $\check{\Sigma}$ , and  $\check{W}$  are respectively the reduced order left singular vectors, singular value matrix, and right singular vectors. The SVD-based EDMD [31] is then carried out as

$$Z_{k+1} = KZ_k; \quad \check{K} = \check{V}^T Z_{k+1} \check{W} \check{\Sigma}^{-1} = \check{V}^T K \check{V} \quad (13)$$

$$\check{K}E = E\Lambda; \quad \Phi = \check{V}E \quad (14)$$

$$b_0 = \Phi^+ [z_0^T \ h(z_0)^T]^T; \quad [z_k^T \ h(z_k)^T]^T = \Phi \Lambda^k b_0 \quad (15)$$

where  $K$  is the approximated Koopman operator, which is equivalently the state matrix;  $E$  and  $\Lambda$  are the eigenvectors and eigenvalues of  $\check{K}$ , respectively. Hence, the model of  $y_1$  and  $y_2$  can be established with Eq.(13-14), and the prediction is carried out by Eq.(15). For regression of both periodic and quasiperiodic sys-

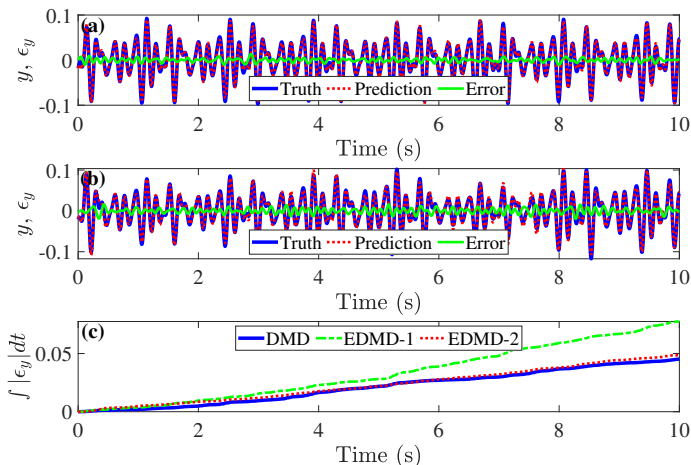


**FIGURE 9:** Prediction of tremor trajectory with EDMD in a 10-second window, where (a) and (b) shows the prediction and error of  $y_1$  and  $y_2$ , respectively; and (c) shows the comparison of three different modeling setup in integral of error norm over time.

tems, 37.5% of the signal data is used for modeling. The modeling setups of a total of four different tests are listed in Tab.1. In particular, different setups are compared for modeling  $y_2$ , which includes a linear DMD, and two EDMD with different delay dimensions. Note that DMD and EDMD-1 have the same total dimension, but DMD covers a larger delay domain.

The results shown in Fig.9 indicate that EDMD effectively regresses both  $y_1$  and  $y_2$ . The reduced-order modes have captured the dominant features in the periodic and quasiperiodic signals. Figure 9(c) shows that the integral of prediction error norm over time is significantly smaller compared to those in Fig.6(c). It is also shown that DMD outperforms EDMD-1 in the integral of prediction error norm over time, which is likely a result of EDMD-1 having a small delay dimension  $m$ . However, by slightly increasing  $m$ , EDMD-2 is able to obtain a prediction performance similar to that of DMD. This shows that by involving nonlinear measurements that potentially match the nonlinear dynamics of tremor, EDMD can achieve good prediction performance with a smaller delay domain. Similar to LSTM-RNN, the results again indicate that such periodic and quasiperiodic solutions can only be acquired in high order systems. The EDMD also provides more physically meaningful information, since the approximated Koopman operator also contains the modes and frequencies of the dynamical system.

### Conclusion and Future Work

This paper studied the data-driven modeling of periodic and quasiperiodic pathological tremor. The observations on the periodicity, frequency component, and chaotic properties of the tremorous movement data confirmed the nonlinearity of the signal. The limitations of the existing tremor prediction model have also been observed from simulations. Based on the general model setup in Eq.(1) and assumption (A1), (A2), the modeling

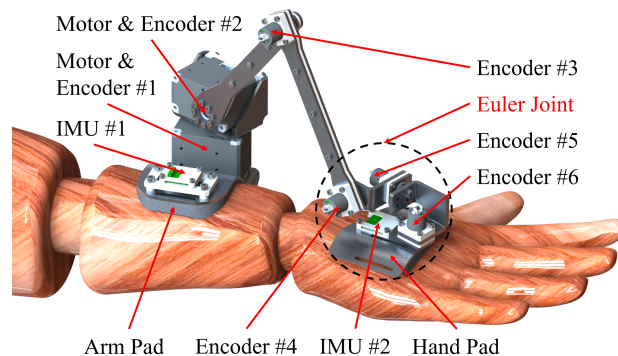


**FIGURE 10:** The design of TAWEx - a tremor alleviating wrist exoskeleton developed by our team [10].

of the tremor signal  $y_1$  (periodic) and  $y_2$  (quasi-periodic) were carried out with LSTM-RNN and EDMD. The results showed that both methods can effectively regress and predict the periodic and quasiperiodic tremor signals in long term, unlike previous methods employed in the literature (e.g., BMFLC and AR), which are only effective for short term prediction.

However, both LSTM-RNN and EDMD are complex and computationally expensive. Also, the data used in this study have very limited information. As such, for future work, we plan to collect more data from experiments and then used these data to construct simpler and more accurate models of pathological tremors. The measurements will include EEG and EMG signals, which respectively correspond to the observations of  $\gamma$  and  $\eta$  from Eq.(1). Also, better multi-dimensional movement measurements will be collected using the tremor suppression exoskeletons developed by our team as shown in Fig.10 [10].

As for data-driven modeling, we will focus on model-based regression and adopt sparsity-based modeling techniques. Note that the complexity of the LSTM-RNN and EDMD is due to a large number of parameters. Sparsity based methods [32] can lead to a simpler model with fewer parameters, which is more feasible for nonlinear analysis. The ultimate goal is to obtain a precise neuromusculoskeletal model that can be used for both nonlinear analysis and real-time long term tremor prediction.

### REFERENCES

- [1] Kalia, L. V., and Lang, A. E., 2015. "Parkinson's disease". *The Lancet*, **386**(9996), pp. 896 – 912.
- [2] Benito-Leon, J., and Louis, E. D., 2006. "Essential tremor: emerging views of a common disorder". *Nature Reviews Neurology*, **2**(12), p. 666.
- [3] McAuley, J., and Marsden, C., 2000. "Physiological and pathological tremors and rhythmic central motor control". *Brain*, **123**(8), pp. 1545–1567.
- [4] Vernooij, C. A., Reynolds, R. F., and Lakie, M., 2013. "A dominant role for mechanical resonance in physiological finger tremor revealed by selective minimization of vol-

- untary drive and movement”. *Journal of neurophysiology*, **109**(9), pp. 2317–2326.
- [5] Bhidayasiri, R., 2005. “Differential diagnosis of common tremor syndromes”. *Postgraduate medical journal*, **81**(962), pp. 756–762.
- [6] Zhang, D., Poignet, P., Widjaja, F., and Ang, W. T., 2011. “Neural oscillator based control for pathological tremor suppression via functional electrical stimulation”. *Control Engineering Practice*, **19**(1), pp. 74–88.
- [7] Heo, J.-H., Kim, J.-W., Kwon, Y., Lee, S.-K., Eom, G.-M., Kwon, D.-Y., Lee, C.-N., Park, K.-W., and Manto, M., 2015. “Sensory electrical stimulation for suppression of postural tremor in patients with essential tremor”. *Bio-medical materials and engineering*, **26**(s1), pp. S803–S809.
- [8] Rocon, E., Belda-Lois, J., Ruiz, A., Manto, M., Moreno, J. C., and Pons, J. L., 2007. “Design and validation of a rehabilitation robotic exoskeleton for tremor assessment and suppression”. *IEEE Transactions on neural systems and rehabilitation engineering*, **15**(3), pp. 367–378.
- [9] Loureiro, R. C., Belda-Lois, J. M., Lima, E. R., Pons, J. L., Sanchez-Lacuesta, J. J., and Harwin, W. S., 2005. “Upper limb tremor suppression in adl via an orthosis incorporating a controllable double viscous beam actuator”. In 9th International Conference on Rehabilitation Robotics, 2005. ICORR 2005., Ieee, pp. 119–122.
- [10] Wang, J., Barry, O., Kurdila, A. J., and Vijayan, S. “On the dynamics and control of a full wrist exoskeleton for tremor alleviation”. In ASME 2019 Dynamic Systems and Control Conference, American Society of Mechanical Engineers Digital Collection.
- [11] Riviere, C. N., Rader, R. S., and Thakor, N. V., 1998. “Adaptive cancelling of physiological tremor for improved precision in microsurgery”. *IEEE Transactions on Biomedical Engineering*, **45**(7), pp. 839–846.
- [12] Veluvolu, K. C., and Ang, W. T., 2011. “Estimation of physiological tremor from accelerometers for real-time applications”. *Sensors*, **11**(3), pp. 3020–3036.
- [13] Tatinati, S., Veluvolu, K. C., Hong, S.-M., Latt, W. T., and Ang, W. T., 2013. “Physiological tremor estimation with autoregressive (ar) model and kalman filter for robotics applications”. *IEEE Sensors Journal*, **13**(12), pp. 4977–4985.
- [14] Seth, A., Hicks, J. L., Uchida, T. K., Habib, A., Dembia, C. L., Dunne, J. J., Ong, C. F., DeMers, M. S., Rajagopal, A., Millard, M., et al., 2018. “Opensim: Simulating musculoskeletal dynamics and neuromuscular control to study human and animal movement”. *PLoS computational biology*, **14**(7), p. e1006223.
- [15] Millard, M., Uchida, T., Seth, A., and Delp, S. L., 2013. “Flexing computational muscle: modeling and simulation of musculotendon dynamics”. *Journal of biomechanical engineering*, **135**(2), p. 021005.
- [16] Valero-Cuevas, F. J., Hoffmann, H., Kurse, M. U., Kutch, J. J., and Theodorou, E. A., 2009. “Computational models for neuromuscular function”. *IEEE Reviews in Biomedical Engineering*, **2**, pp. 110–135.
- [17] He, J., Maltenfort, M. G., Wang, Q., and Hamm, T. M., 2001. “Learning from biological systems: Modeling neural control”. *IEEE Control Systems Magazine*, **21**(4), pp. 55–69.
- [18] Sartori, M., Lloyd, D. G., and Farina, D., 2016. “Neural data-driven musculoskeletal modeling for personalized neurorehabilitation technologies (vol 63, pg 879, 2016)”. *IEEE TRANSACTIONS ON BIOMEDICAL ENGINEERING*, **63**(6), pp. 1341–1341.
- [19] Zhang, D., Poignet, P., Bo, A. P., and Ang, W. T., 2009. “Exploring peripheral mechanism of tremor on neuromusculoskeletal model: A general simulation study”. *IEEE Transactions on Biomedical Engineering*, **56**(10), pp. 2359–2369.
- [20] Lakie, M., Vernooij, C. A., Osborne, T. M., and Reynolds, R. F., 2012. “The resonant component of human physiological hand tremor is altered by slow voluntary movements”. *The Journal of physiology*, **590**(10), pp. 2471–2483.
- [21] Isenkul, M., Sakar, B., and Kursun, O., 2014. “Improved spiral test using digitized graphics tablet for monitoring parkinson’s disease”. In Proc. of the Int’l Conf. on e-Health and Telemedicine, pp. 171–5.
- [22] Hochberg, L. R., Serruya, M. D., Friebs, G. M., Mukand, J. A., Saleh, M., Caplan, A. H., Branner, A., Chen, D., Penn, R. D., and Donoghue, J. P., 2006. “Neuronal ensemble control of prosthetic devices by a human with tetraplegia”. *Nature*, **442**(7099), p. 164.
- [23] Campbell, S. A., 2007. “Time delays in neural systems”. In *Handbook of brain connectivity*. Springer, pp. 65–90.
- [24] Palanhandalam-Madapusi, H. J., and Goyal, S., 2011. “Is parkinsonian tremor a limit cycle?”. *Journal of Mechanics in Medicine and Biology*, **11**(05), pp. 1017–1023.
- [25] Singh, G. K., Shah, V. V., and Palanhandalam-Madapusi, H. J., 2013. “Diagnosis of parkinson’s disease: A limit cycle approach”. In 2013 IEEE International Conference on Control Applications (CCA), IEEE, pp. 252–257.
- [26] Rosenstein, M. T., Collins, J. J., and De Luca, C. J., 1993. “A practical method for calculating largest lyapunov exponents from small data sets”. *Physica D: Nonlinear Phenomena*, **65**(1-2), pp. 117–134.
- [27] Haykin, S. S., 2005. *Adaptive filter theory*. Pearson Education India.
- [28] Yilmaz, G., Ugan, P., Sebik, O., Uginčius, P., and Türker, K. S., 2014. “Interference of tonic muscle activity on the eeg: a single motor unit study”. *Frontiers in human neuroscience*, **8**, p. 504.
- [29] Gers, F. A., Eck, D., and Schmidhuber, J., 2002. “Applying lstm to time series predictable through time-window

- approaches”. In *Neural Nets WIRN Vietri-01*. Springer, pp. 193–200.
- [30] Williams, M. O., Kevrekidis, I. G., and Rowley, C. W., 2015. “A data-driven approximation of the koopman operator: Extending dynamic mode decomposition”. *Journal of Nonlinear Science*, **25**(6), pp. 1307–1346.
- [31] Proctor, J. L., Brunton, S. L., and Kutz, J. N., 2016. “Dynamic mode decomposition with control”. *SIAM Journal on Applied Dynamical Systems*, **15**(1), pp. 142–161.
- [32] Loiseau, J.-C., and Brunton, S. L., 2018. “Constrained sparse galerkin regression”. *Journal of Fluid Mechanics*, **838**, pp. 42–67.